EUROPEAN JOURNAL OF
CARDIO-THORACIC
SURGERY

Ultrastructural changes in pneumocyte type II cells following traumatic brain injury in rats

Erkan Yildirim, Erkan Kaptanoglu, Kanat Ozisik, Ethem Beskonakli, Ozerk Okutan, Mustafa F. Sargon, Kamer Kilinc and Unal Sakinci

Eur J Cardiothorac Surg 2004;25:523-529
DOI: 10.1016/j.ejcts.2003.12.021

ELSEVIER

European Journal of Cardio-thoracic Surgery 25 (2004) 523–529

EUROPEAN JOURNAL OF CARDIO-THORACIC SURGERY

www.elsevier.com/locate/ejcts

Ultrastructural changes in pneumocyte type II cells following traumatic brain injury in rats☆

Erkan Yildirim[a,*], Erkan Kaptanoglu[b], Kanat Ozisik[a], Ethem Beskonakli[b], Ozerk Okutan[b], Mustafa F. Sargon[c], Kamer Kilinc[d], Unal Sakinci[a]

[a]*Department of Thoracic Surgery, Ankara Numune Education and Research Hospital, Ankara, Turkey*
[b]*Department of Neurosurgery, Ankara Numune Education and Research Hospital, Ankara, Turkey*
[c]*Department of Anatomy, Faculty of Medicine, Hacettepe University, Ankara, Turkey*
[d]*Department of Biochemistry, Faculty of Medicine, Hacettepe University, Ankara, Turkey*

Received 23 July 2003; received in revised form 4 October 2003; accepted 15 December 2003

Abstract

Objective: We aimed to demonstrate the time-dependent ultrastructural changes in pneumocyte type II cells following brain injury, and to propose an electron microscopic scoring model for the damage. **Methods**: Forty Wistar-Albino female rats weighing 170–200 g were used. The rats were allocated into five groups. The first group was the control and the second was the craniotomy without trauma. The others were trauma groups. Weight-drop method was used for achieving head trauma. Samples were obtained from the right and left pulmonary lobes at 2-, 8-, and 24-h intervals after transcardiac perfusion. An electron microscopic scoring model was used to reveal the changes. **Results**: There were no ultrastructural pathological findings pointing to lung injury in any rat of the control groups. There was intense intracellular oedema in type II pneumocyte and interstitial oedema in the adjacent tissue in trauma groups. Oedema in mitochondria and dilatation in both smooth endoplasmic reticulum and Golgi apparatus was more evident in the 8- and 24-h trauma groups. The chromatin dispersion was disintegrated in the nucleus in all trauma groups. Scores of all trauma groups were significantly different from the controls ($P < 0.05$). All trauma groups were different from each other at significant levels ($P < 0.05$ for each trauma groups). **Conclusions**: The data suggested that ultrastructural damage is obvious at 2 h and deteriorates with time. The electron microscopic scoring model worked well in depicting the traumatic changes, which were supported by lipid peroxidation. Further experiments are needed to determine the exact outcome after brain death model.

Keywords: Brain; Trauma; Animal model; Electron microscopy; Lung; Pneumocyte type II cells

1. Introduction

Blunt traumatic brain injury represents one of the most important causes of death and disability in modern society [1]. Acute lung injury is common in comatose victims with an isolated traumatic brain injury and is associated with an increased risk of death or a severe neurological morbidity [2]. Traumatic brain injury often leads to severe reduction in blood flow, which is one of the most important causes of secondary brain damage [3]. Cerebral hypoxia or ischemia and head trauma or seizures may all lead to severe neurogenic pulmonary injury [4–6]. It is difficult to diagnose neurogenic pulmonary oedema and exact pathophysiology is not completely understood [7,8].

There are several theories on how neurogenic pulmonary oedema occurs, such as the blast theory [9], the permeability defect theory, constriction of lymphatics and pulmonary microembolisation [10]. The relative contribution of hydrostatic and permeability mechanisms to the development of human neurogenic pulmonary oedema has been identified [5,7,11]. Although the mediators of the permeability defect and the critical central nervous system structures are unknown, the medulla and the hypothalamus have been suggested as likely contributors to the disease process [2,8]. Sympathetic hyperactivity during sudden

☆ Presented at the Joint 17th Annual Meeting of the European Association for Cardio-thoracic Surgery and the 11th Annual Meeting of the European Society of Thoracic Surgeons, Vienna, Austria, October 12–15, 2003.

* Corresponding author. Address: Asagiovecler Mh. 79.Sk. 8/3 Dikmen, Cankaya, Ankara, Turkey. Tel.: +90-312-482-72-79; fax: +90-312-310-34-60.

E-mail address: erseyda@yahoo.com (E. Yildirim).

1010-7940/$ - see front matter © 2004 Elsevier B.V. All rights reserved.
doi:10.1016/j.ejcts.2003.12.021

intracranial hypertension leads to cardiovascular instability, myocardial dysfunction, and neurogenic pulmonary oedema [7,12]. Free radicals coming out after central nervous system injury may also contribute to the formation of neurogenic pulmonary oedema [8]. It seems that neurogenic pulmonary oedema is probably the result of a combination of all the pathways mentioned above.

Neurogenic pulmonary oedema has also been linked with adult respiratory distress syndrome. Indeed it is rare; neurogenic pulmonary oedema may occur within minutes to hours of the central nervous system injury, or it may have a delayed onset, occurring days later [7,8].

Results of some animal studies have shown a relation between acute brain injury and pulmonary oedema in the absence of underlying cardiac and pulmonary diseases [5,8].

In the current study, we intended mainly to demonstrate the effects of traumatic brain injury on lung parenchyma on the organelles of type II pneumocyte and alveolocapillary membrane where the vital oxygenation takes place in a time-dependent manner. The secondary aim was to suggest an ultrastructural scoring system to evaluate the degree of damage in the lung after traumatic brain injury.

2. Materials and methods

All animals received humane care in compliance with the European Convention on Animal Care. The local Institutional Animal Care Committee approved protocols used in this study.

2.1. Experimental groups

Forty female Wistar–Albino rats were randomly allocated into five groups:

- Group 1 (G1) Control group ($n = 8$) : Tissue samples were obtained immediately after thoracotomy and no head surgery was performed.
- Group 2 (G2) Sham operated group ($n = 8$) : Scalp was closed after craniotomy and no trauma was induced. Tissue samples were obtained 24 h after surgical interventions.
- Group 3 (G3) Trauma 2-h group ($n = 8$) : Impact of 140 g-cm brain injuries was produced. Tissue samples were obtained 2 h after trauma.
- Group 4 (G4) Trauma 8-h group ($n = 8$) : Impact of 140 g-cm brain injuries was produced. Tissue samples were obtained 8 h after trauma.
- Group 5 (G5) Trauma 24-h group ($n = 8$) : Impact of 140 g-cm brain injuries was produced. Tissue samples were obtained 24 h after trauma.

2.2. Surgical procedure

The surgical procedure was performed under general anaesthesia induced by 10 mg/kg xylasine (Bayer, Istanbul, Turkey) and 60 mg/kg ketamine hydrochloride (Parke Davis, Istanbul, Turkey) intramuscularly. Forty rats, weighing 170–200 g were placed in prone position. Following midline longitudinal incision, scalp was dissected over cranium and retracted laterally. Coronal and sagittal sutures were observed. Right frontoparietal craniectomies were carried out lateral to the sagittal suture by dental drill system. The dura was exposed and left intact. Trauma of 140 g-cm impacts was produced by the method of Allen [13]. Rats were injured by a stainless steel rod (5 mm diameter, weighing 140 g) weight dropped vertically through a calibrated tube from a height of 10 cm onto the exposed dura. Scalp was sutured with silk sutures. Body temperature was continuously monitored during the whole procedure with a rectal thermometer and maintained at 37 °C using a heating pad and an overhead lamp. Rats were neither intubated nor ventilated between brain damage and lung sampling. They were given free access to food and water.

2.3. Obtaining samples from lung parenchyma

Two, 8, and 24 h after traumatic brain injury for trauma groups and 24 h after sham operation for sham group, rats were re-anaesthetized with the combination of ketamine and xylasine. Rats were placed supine on the operating table. Midline sternotomy and bilateral thoracotomy were performed. The systemic circulation was perfused with 0.9% NaCl. Samples for lipid peroxidation and electron microscopy were obtained from the right and the left pulmonary lobes concurrently. Then, rats were killed by decapitation under general anaesthesia. Lung samples were collected in randomly numbered containers and given to the blinded observers. After evaluating the numbered tissues, results were collected in the appropriate group lists.

2.4. Transmission electron microscopy

The specimens were fixed in 2.5% gluteraldehyde for 24 h, washed in phosphate buffer (pH 7.4), post-fixed in 1% osmium tetroxide in phosphate buffer (pH 7.4) and dehydrated in increasing concentrations of alcohol. Then the tissues were washed with propylene oxide and embedded in epoxy-resin embedding media. Semi-thin sections about 2 μm in thickness and ultra thin sections about 60 nm in thickness were cut with a glass knife on an LKB-Nova (Sweden) ultramicrotome. Semi-thin sections were stained with methylene blue and examined by a Nikon Optiphot (Japan) light microscope. Ultrathin sections were collected on copper grids, stained with uranyl acetate and lead citrate and examined with a Joel JEM 1200 EX (Japan) transmission electron microscope.

Ultrastructural data were evaluated based on each sub cellular change and the data were collected and estimated as lung injury score (modified from a study of Kaptanoglu et al. [14]; Table 1).

2.5. Lipid peroxidation assay

The samples were thoroughly cleansed of blood and were immediately frozen and stored in a − 20 °C freezer for assays of malondialdehyde. The levels of lipid peroxidation were measured as thiobarbituric acid-reactive material. The level of lipid peroxidation in the lung parenchyma was determined using the method of Mihara and Uchiyama [15]. Tissues were homogenized in 10 volumes (w/v) of cold phosphate buffer (pH 7.4). Half a millilitre of homogenate was mixed with 3 ml 1% H_3PO_4. After the addition of 1 ml 0.67% thiobarbituric acid, the mixture was heated in boiling water for 45 min. The colour was extracted into *n*-butanol, and the absorption at 532 nm was measured. Using tetramethoxy-propane as the standard, tissue lipid peroxidation levels were calculated as nanomole per gram of wet tissue.

2.6. Statistical analysis

All the data collected from the experiment were coded, recorded, and analysed by using SPSS 10.0.1 for Windows. ANOVA for parametric data and Kruskal–Vallis variance test for non-parametric data were used for comparing differences between groups. When analysis of variance showed a significant difference, the post-hoc multiple comparison test was applied to demonstrate the differences in the groups. In each test, the data were expressed as the mean value ± standard error (SE) and $P < 0.05$ were accepted as statistically significant.

3. Results

There were no differences determined between the right and left pulmonary lobes. The alveolocapillary membrane was intact, and no ultrastructural changes were detected in type I pneumocyte cells in any groups. Additionally, there was no lymphocyte infiltration in any groups. Granular endoplasmic reticulum was not affected in any trauma groups.

3.1. Transmission electron microscopy (scoring)

There were no ultrastructural pathological findings determined in the control (G1) and sham (G2) groups (Fig. 1a and b).

In 2-h trauma (G3) group, there was intense intracellular oedema in type II pneumocyte. Additionally, oedema in mitochondria and dilatation in both smooth endoplasmic reticulum and Golgi apparatus were determined. The chromatin dispersion was disintegrated in the nucleus and the chromatin was clustered peripherally in places (Fig. 2a–c).

In 8-h trauma (G4) group, there was intense intracellular vacuoles in type II pneumocyte. There was also oedema in the mitochondria and dilatations in smooth endoplasmic reticulum and Golgi apparatus. The chromatin dispersion was disintegrated in the nucleus and the chromatin was clustered peripherally in places (Fig. 3a and b).

In 24-h trauma (G5) group, there was intense intracellular vacuoles in type II pneumocyte similarly as the previous trauma groups. There was evident oedema in the mitochondria and dilatations in smooth endoplasmic reticulum and Golgi apparatus. The chromatin dispersion was disintegrated in the nucleus and the chromatin was clustered peripherally in places (Fig. 4a and b).

3.2. Lipid peroxidation assay

There was statistically significant difference between the 24-h and other groups ($P < 0.05$). Traumatic brain injury increased lung tissue lipid peroxidation levels significantly at 24 h after trauma.

There was no statistical difference between control, sham, 2- and 8-h groups ($P > 0.05$; Fig. 5).

Table 1
Lung injury scores

Grade\organelle	N	GER	SER	M	IV
0	Normal	Normal	Normal	Normal	Normal
1	Disintegrated chromatin (margination, clumping)	Dilated	Dilated in places	Clear cristae	Small
2	Increased hetero-chromatin	Corrupted lamellar arrangement	Existing vacuoles	Oedematous	Middle
3	Degenerated nucleuses	Broken	Fields of broad degeneration + myelin figures	Accumulation of amorphous material	Large

Lung injury is scored as grades of injury (0, 1, 2, and 3), and evaluated separately in each organelle of pneumocyte type II cells. Abbreviations: N, nucleus; GER, granulated endoplasmic reticulum, SER, smooth endoplasmic reticulum; M, mitochondria; IV, intracytoplasmic vacuoles.

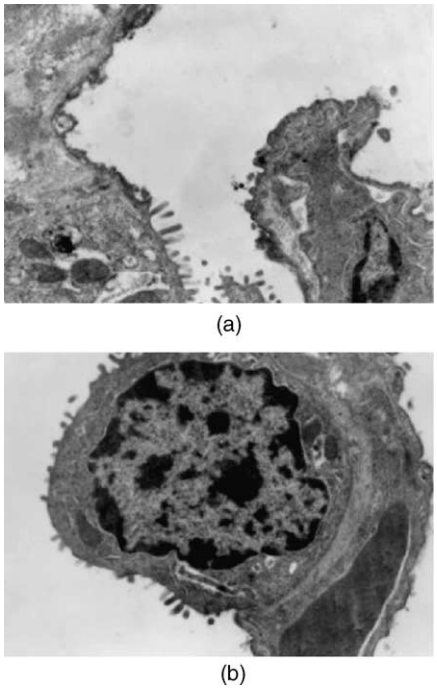

Fig. 1. (a) Electron micrograph showing no ultrastructural pathologic findings determined in control group (G1; original magnification × 10 000). (b) Electron micrograph showing no ultrastructural pathologic findings determined in sham group (G2; original magnification × 10 000).

3.3. Statistical analyses of the organelles of pneumocyte type II cells

3.3.1. Intracytoplasmic vacuoles

Two-, 8- and 24-h groups showed statistical difference from control and sham groups ($P < 0.05$). There was no statistically significant difference between 2- and 8-h groups ($P > 0.05$). Twenty-four hour group showed the worst results and significant difference was observed from all other groups ($P < 0.05$).

3.3.2. Nucleus

All the trauma groups showed increased nuclear damage statistically significant levels comparing to control and sham groups ($P < 0.05$). There was statistically significant difference between 2- and 8-h groups ($P < 0.05$), and 2- and 24-h groups ($P < 0.05$). There was no statistically significant difference between 8- and 24-h groups ($P > 0.05$).

3.3.3. Smooth endoplasmic reticulum

Score of the trauma groups was significantly different from control and sham groups ($P < 0.05$). There was statistical difference between 2-, 8- and 24-h groups ($P < 0.05$). Trauma produced obvious damage to the ultrastructure of the smooth endoplasmic reticulum in time-dependent manner. All trauma groups were different from each other in significant levels ($P < 0.05$ for each trauma groups).

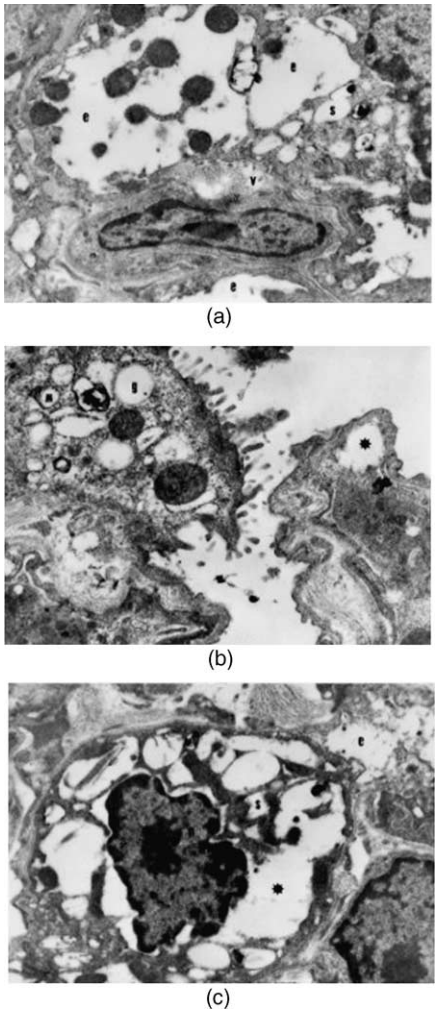

Fig. 2. (a) Electron micrograph showing initial ultrastructural pathologic findings starting in 2-h trauma group (G3). Interstitial oedema in the adjacent tissue (e), dilated smooth endoplasmic reticulum (s), and vacuoles in capillary endothelial cells (v) were shown (original magnification × 7500). (b) Electron micrograph showing dilatation of Golgi apparatus (g), oedematous mitochondria (m), and intracellular vacuole (*) in 2-h trauma group (G3; original magnification × 10 000). (c) Electron micrograph showing chromatin dispersion located peripherally in places (n), dilated smooth endoplasmic reticulum (s), oedematous mitochondria (m), interstitial oedema in the adjacent tissue (e), and intracellular vacuole (*) in 2-h trauma group (G3; original magnification × 10 000).

3.3.4. Granular endoplasmic reticulum

No damage was observed in the granular endoplasmic reticulum in all groups.

3.3.5. Mitochondrion

All trauma groups were significantly different from controls ($P < 0.05$). Gradual mitochondrial damage was observed in trauma groups ($P < 0.05$).

3.3.6. General score of lung injury score

There was no statistical difference between control and sham operated animals ($P > 0.05$). Scores of all trauma

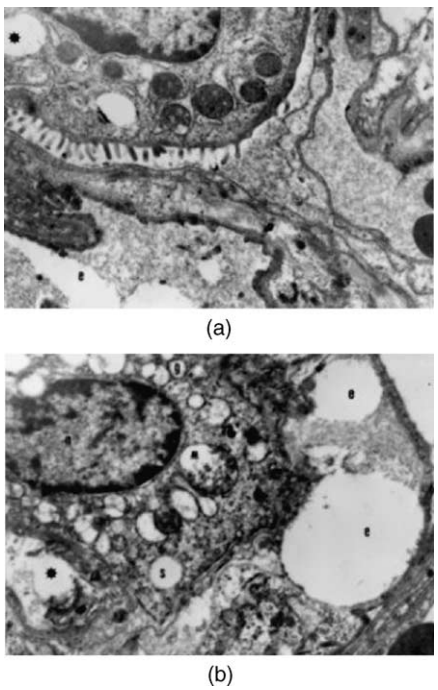

Fig. 3. (a) Electron micrograph showing ultrastructural pathologic findings deteriorating in group of 8-h trauma (G4). There were intense intracellular vacuoles (*), and interstitial oedema in the adjacent tissue (e) (original magnification × 7500). (b) Electron micrograph showing oedema in the mitochondria (m), and dilatations in smooth endoplasmic reticulum (s) and Golgi apparatus (g) in group of 8-h trauma (G4). The chromatin dispersion was disintegrated in the nucleus and the chromatin was clustered peripherally in places (n). There were intracellular vacuoles (*) and oedematous mitochondria in the capillary endothelial cells (original magnification × 10 000).

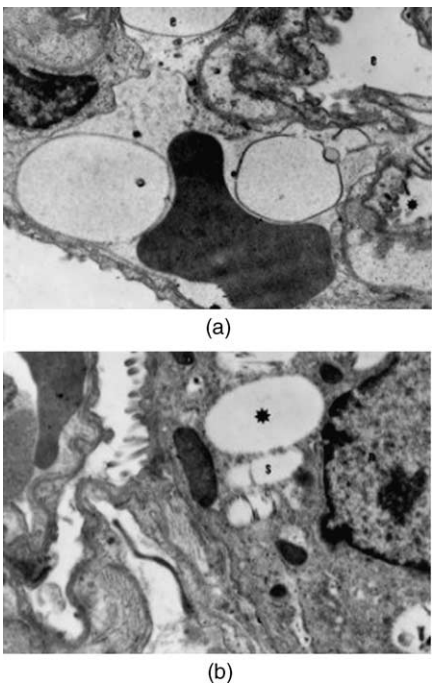

Fig. 4. (a) Electron micrograph showing ultrastructural pathologic findings getting worst in the group of 24-h trauma group (G5). There was intense intracellular vacuoles (*), and interstitial oedema in the adjacent tissue (e) (original magnification × 7500). (b) Electron micrograph showing oedema in the mitochondria (m), and dilatations in smooth endoplasmic reticulum (s) and Golgi apparatus in 24-h trauma group (G5). The chromatin dispersion was more prominently disintegrated in the nucleus and the chromatin was clustered peripherally in places (n). Abbreviations: *, intracellular vacuole; e, interstitial oedema in the adjacent tissue; m, oedematous mitochondria; s, dilated smooth endoplasmic reticulum; g, dilatation of Golgi apparatus; v, vacuoles in capillary endothelial cells; n, nucleus. Magnification × 7500–10 000, bar represents 1 μm.

groups were significantly different from the controls ($P < 0.05$). All trauma groups were different from each other in significant levels ($P < 0.05$ for each trauma groups). Trauma produced obvious gradual damage on the ultrastructure of the lung in time-dependent manner. Results of lung injury score were shown in Fig. 6.

4. Discussion

Our results showed that traumatic brain injury caused pathological changes in lung tissue that transmission electron microscopy clearly documented. The ultrastructural damage started to appear slightly in the 2-h trauma group and then deteriorated through the study and got worse apparently in the 24-h trauma group. Simultaneously, the lipid peroxidation levels were significantly higher in trauma group than the control and sham groups, which also supported the existence of pathological findings, frankly.

The principal pathophysiological processes in acute central nervous system injury, such as stroke, mechanical trauma, or subarachnoid haemorrhage, are extremely complex and involve pathological permeability of blood brain barrier, energy failure, loss of cell ion homeostasis. And additionally, acidosis, increased intracellular calcium, excitotoxicity, increased neurotransmitters and free radical-mediated toxicity may contribute this complex phenomenon [4–6,8,11]. Structural changes and glial injury occur due to

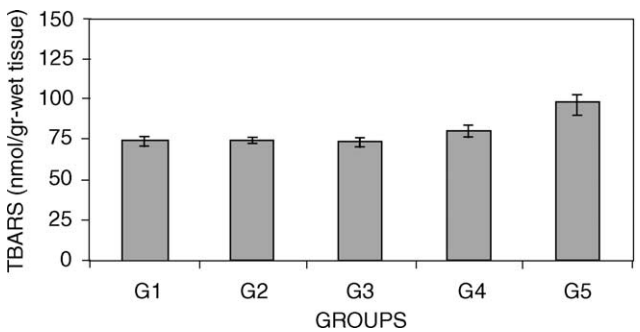

Fig. 5. Figure shows the effect of traumatic brain injury on lung TBARS levels. Traumatic brain injury increased lung tissue lipid peroxidation levels significantly at especially 24 h. A mean value of the TBARS levels of the lung tissue is presented as bars and standard error of the mean is presented as vertical lines. TBARS content of the lung is expressed as nmol TBARS/g-wet tissue, mean ± SE. TBARS; thiobarbituric acid reactive substances.

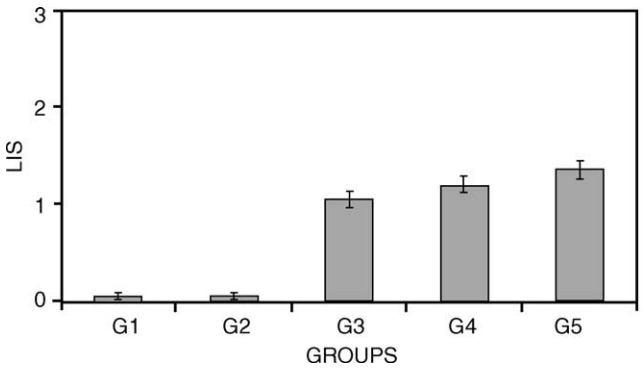

Fig. 6. There was statistically difference between G3, G4 and G5 groups regarding lung injury score ($P < 0.05$). Trauma produced obvious gradual damage on ultrastructure of the lung in a time-dependent manner more prominent in 24-h trauma group. Abbreviations: G1, control group; G2, sham group; G3, 2-h trauma group; G4, 8-h trauma group; G5, 24-h trauma group.

free radicals [8,11]. Traumatic brain injury stimulates oxygen radical production and is associated with cerebral blood flow reduction [3]. Moreover, radicals can cause damage to cardinal cellular components such as lipids, proteins, and nucleic acids [11].

On the other hand, sympathetic hyperactivity during central nervous system events leads to cardiovascular instability and neurogenic pulmonary oedema [7,12]. Massive sympathetic discharge following traumatic brain injury causes both pulmonary and systemic vasoconstrictions. This causes increase in both pulmonary blood pressure and left atrial pressure causing increase of pulmonary capillary pressure. The resultant pulmonary capillary damage causes alteration in capillary permeability. The outcome is acute pulmonary oedema [5,7,16]. But, indeed the pathophysiology of neurogenic pulmonary oedema is not yet well defined [8].

It seems there is not a single mechanism to be accepted occurring after brain injury as stated in detail above.

Wang et al. [17] studied ultrastructural changes of Clara and type II alveolar cells. In the early 1970s, an electron microscopic study on the alterations at the alveolar level in pulmonary oedema was published [18].

In the present study, the time-dependent ultrastructural changes after experimental traumatic brain injury were demonstrated using a promising scoring model [14] for graded injury in type II pneumocyte. The deteriorating changes were scored as 0, 1, 2, and 3 grades with differing explanations according to the organelles studied. In addition, intracellular vacuoles were defined due to their changing sizes.

Oxygen radical formation after trauma results in cell membrane lipid peroxidation causing membrane lyses [14]. Substantial amount of lipid peroxidation in traumatically injured brain is generated [3], and it takes place during the first 30–60 min after injury [3,19]. Besides ultrastructural damage, we also determined that the traumatic brain injury increased lung tissue lipid peroxidation levels significantly, particularly at post-trauma 24-h group ($P < 0.05$).

Brainstem death develops in most multiorgan donors as a result of spontaneous intracerebral bleeding or severe head injury. The composition, function, and metabolism of pulmonary surfactant produced by alveolar type II cells are increasingly being recognized as important factors in pulmonary ischemia–reperfusion injury. Reperfusion after a period of pulmonary ischemia results in significant endothelial and alveolar type II cell dysfunction [20]. This may result in disturbed oxygen exchange due to collapse related to impaired function of type II pneumocyte. This phenomenon may be the cause of higher morbidity and lower graft survival rates in the world of organ shortage where almost half of the organ donors have deceased from head trauma [21].

In conclusion, the traumatic brain injury caused clearly ultrastructural damage in type II pneumocyte. The pathological findings were depicted in detail according to the organelles by using a newly suggested electron microscopic grading model. Lipid peroxidation levels supported the presence of damage in type II pneumocyte. In the light of the facts, it is of paramount importance to harvest the lungs at the earliest possible time.

Further studies are required to determine the ultrastructural pathological changes in pneumocyte type II cells and at its product, surfactant, after more severe brain injury or death.

References

[1] Siegel JH, Gens DR, Mamantov T, Geisler FH, Goodarzi S, MacKenzie EJ. Effect of associated injuries and blood volume replacement on death, rehabilitation needs, and disability in blunt traumatic brain injury. Crit Care Med 1991;19(10):1252–65.
[2] Bratton SL, Davis RL. Acute lung injury in isolated traumatic brain injury. Neurosurgery 1997;40:707–12.
[3] Hoffman SW, Moore S, Ellis EF. Isoprostanes: free radical-generated prostaglandins with constrictor effects on cerebral arterioles. Stroke 1997;28:844–9.
[4] Edmonds Jr. HL, Cannon Jr. HC, Garretson HD, Dahlquist G. Effects of aerosolised methylprednisolone on experimental neurogenic pulmonary injury. Neurosurgery 1986;19:36–40.
[5] Maron MB. Effect of elevated vascular pressure transients on protein permeability in the lung. J Appl Physiol 1989;67(1):305–10.
[6] Schwarz S, Schwab S, Keller E, Bertram M, Hacke W. Neurogene störungen der herz-und lungenfunktion bei akuten zerebralen läsionen. Nervenartz 1997;68:956–62.
[7] Pyeron AM. Respiratory failure in the neurological patient: the diagnosis of neurogenic pulmonary oedema. J Neurosci Nurs 2001;33(4):203–7.
[8] Dettbarn CL, Davidson LJ. Pulmonary complications in the patient with acute head injury: neurogenic pulmonary oedema. Heart Lung 1989;18:583–9.
[9] Smith WS, Matthay MA. Evidence for a hydrostatic mechanism in human neurogenic pulmonary oedema. Chest 1997;111:1326–33.
[10] Singbartl G. Kardio-zirkulatorische und pulmonale Veränderungen bei patienten mit isolierter zerebraler Läsion. Anaesthetist 1989;38:360–74.

[11] Gilgun-Sherki Y, Rosenbaum Z, Melamed E, Offen D. Antioxidant therapy in acute central nervous system injury: current state. Pharmacol Rev 2002;54:271–84.
[12] Hall SR, Wang L, Milne B, Ford S, Hong M. Intrathecal lidocaine prevents cardiovascular collapse and neurogenic pulmonary oedema in a rat model acute intracranial hypertension. Anesth Analog 2002; 94:948–53.
[13] Allen AR. Surgery of experimental lesion of spinal cord equivalent to crush injury of fracture dislocation of spinal column. A preliminary report. J Am Med Assoc 1911;57:878–80.
[14] Kaptanoglu E, Sen S, Beskonakli E, Surucu HS, Tuncel M, Kilinc K, Taskin Y. Antioxidant actions and early ultrastructural findings of thiopental and propofol in experimental spinal cord injury. J Neurosurg Anaesth 2002;14(2):114–22.
[15] Mihara M, Uchiyama M. Evaluation of thiobarbituric acid (TBA) value as an index of lipid peroxidation in CCl4-intoxicated rat liver (author's transl). Yakugaku Zasshi 1981;101(3):221–6.
[16] West JB. Cellular responses to mechanical stress: Invited review: pulmonary capillary stress failure. J Appl Physiol 2000;89:2483–9.
[17] Wang NS, Huang SN, Sheldon H, Thurlbeck WM. Ultrastructural changes of Clara and type II alveolar cells in adrenalin-induced pulmonary oedema in mice. Am J Pathol 1971;62(2):237–52.
[18] Cottrell TS, Levine OR, Senior RM, Wiener J, Spiro D, Fishman AP. Electron microscopic alterations at the alveolar level in pulmonary oedema. Circ Res 1967;21(6):783–97.
[19] Kaptanoglu E, Tuncel M, Palaoglu S, Konan A, Demirpence E, Kilinc K. Comparison of the effects of melatonin and methylprednisolone in experimental spinal cord injury. J Neurosurg (Spine 1) 2000;93:77–84.
[20] Novick RJ, Gehman KE, Ali IS, Lee J. Lung preservation: the importance of endothelial and alveolar type II cell integrity. Ann Thorac Surg 1996;62:302–14.
[21] Corman J, Clermont MJ, Dandavino R, Daloze P, Lachance JG, Mangel R, Corcos J, Chartrand C, Poirier N, Marleau D. Development of organ transplantation in Quebec from 1985 to January 1990. Ann Chir 1991;45(9):791–5.